

# Previous Knowledge Utilization in Online Anytime Belief Space Planning

Michael Novitsky , Moran Barenboim , and Vadim Indelman , *Member, IEEE*

**Abstract**—Online planning under uncertainty remains a critical challenge in robotics and autonomous systems. While tree search techniques are commonly employed to construct partial future trajectories within computational constraints, most existing methods discard information from previous planning sessions considering continuous spaces. This study presents a novel, computationally efficient approach that leverages historical planning data in current decision-making processes. We provide theoretical foundations for our information reuse strategy and introduce an algorithm based on Monte Carlo Tree Search (MCTS) that implements this approach. Experimental results demonstrate that our method significantly reduces computation time while maintaining high performance levels. Our findings suggest that integrating historical planning information can substantially improve the efficiency of online decision-making in uncertain environments, paving the way for more responsive and adaptive autonomous systems.

**Index Terms**—Decision making, Uncertain systems, Monte Carlo methods.

## I. INTRODUCTION

**A**UTONOMOUS agents often operate under uncertainty due to sensor noise and incomplete information, maintaining a belief (probability distribution) over possible states instead of direct access to the true environment state. Partially Observable Markov Decision Processes (POMDPs) provide a framework for such settings, but solving them optimally is computationally intractable (PSPACE-complete) [1], mainly due to the curse of history, curse of dimensionality, and continuous state, action and observation spaces common in real-world applications.

Recent advancements have introduced online algorithms [2], [3], [4] that find approximate solutions to POMDPs. These algorithms operate within limited budget constraints, such as restricted time, and employ a sampling-based approach to construct partial trees and search for the optimal action that maximizes the expected cumulative reward. By sampling a subset of the belief space, these algorithms effectively address both the

curse of history and the curse of dimensionality, which are key obstacles in solving POMDPs.

In POMDPs, the reward function of a belief node is typically formulated as the expected reward over states. However, this formulation may be insufficient for certain problems, such as information gathering and active sensing. In such cases, the problem is commonly addressed as Belief Space Planning (BSP) or  $\rho$ -POMDP [5], where the reward is defined over the belief itself. Information-theoretic measures, such as information gain and differential entropy, are commonly used to quantify uncertainty in the decision-making process [6]. However, exact calculation of information-theoretic rewards becomes intractable for general distributions, as it requires integrating over all possible states. To address this challenge, approximation methods such as kernel density estimation (KDE) and particle filter estimation [7] have been proposed in the literature. Nonetheless, these methods still incur significant computational expenses, with computation complexity scaling quadratically with the number of samples. As reward calculation is performed for each node in the tree, it becomes the primary source of computational complexity in online planning algorithms.

The main objective of this letter is to improve planning efficiency within a non-parametric setting, continuous state, action and observation spaces, and general reward functions. To address these challenges, we contribute a novel approach that leverages the Multiple Importance Sampling framework [8] to tackle the problem of reusing information from previous planning sessions. We demonstrate how our method can be integrated with Monte Carlo Tree Search (MCTS) to create a novel online algorithm called Incremental Reuse Particle Filter Tree (IR-PFT). We evaluate our algorithm in an online planning setting, demonstrating reduced planning time without performance loss.

The code for this letter is available at <https://github.com/miken1990/ir-pft>.

## II. RELATED WORK

Solving POMDPs is challenging, but methods like POMCP [2] and POMCPOW [10] have advanced the field. POMCP extends UCT [9] to partial observability by sampling a state from the current belief, propagating it through a search tree, and recording statistics with a Multi-Armed Bandit for action selection in discrete spaces. POMCPOW adapts this approach to continuous action and observation spaces using progressive widening and weighted particle sets with an observation likelihood model.

Received 3 June 2025; accepted 13 August 2025. Date of publication 4 September 2025; date of current version 15 September 2025. This article was recommended for publication by Associate Editor P. Ogren and Editor M. Vincze upon evaluation of the reviewers' comments. This work was supported by US NSF/US-Israel BSF. (*Corresponding author: Michael Novitsky.*)

Michael Novitsky and Moran Barenboim are with Technion Autonomous Systems Program (TASP), Technion - Israel Institute of Technology, Haifa 32000, Israel (e-mail: miken1990@campus.technion.ac.il; moran-bar@campus.technion.ac.il).

Vadim Indelman is with the Stephen B. Klein Faculty of Aerospace Engineering and Faculty of Data and Decision Sciences, Technion - Israel Institute of Technology, Haifa 32000, Israel (e-mail: vadim.indelman@technion.ac.il).

Digital Object Identifier 10.1109/LRA.2025.3606381

2377-3766 © 2025 IEEE. All rights reserved, including rights for text and data mining, and training of artificial intelligence and similar technologies. Personal use is permitted, but republication/redistribution requires IEEE permission. See <https://www.ieee.org/publications/rights/index.html> for more information.

In PFT-DPW [10] the authors adopt particle filter formulation for belief update and each belief is represented with a constant number of samples.  $\rho$ -POMCP [11] propagates a set of particles in each simulation using a particle filter and adds it to existing particles in visited nodes. Frequently visited nodes achieve better representation, with convergence proven asymptotically for continuous, bounded  $\rho$ .

IPFT [6] extends PFT [10] by incorporating a reward function defined as a linear combination of differential entropy and expected state reward. In each simulation, a particle set is sampled from the root belief and propagated through the tree. Entropy estimates are averaged across particle sets at each belief node to estimate differential entropy.

LABECOP [4] is designed for continuous observation spaces. At each belief node  $b$ , a state  $s$  is sampled, an action  $a$  selected via modified UCB, and an observation  $o$  is sampled. The states for  $b, a$  are reweighted using  $o$  to improve  $\hat{Q}(b, a)$ .

SITH-BSP [12], [13] and AI-FSSS [14] make use of simplification of the reward function calculation and observation space sampling accordingly, while preserving action consistency. The extension of  $\rho$ -POMDP to  $\mathbb{P}\rho$ -POMDP in [15] incorporates stochastic bounds on the return, while also quantifying the effects of applying simplifications.

DESPOT [3] and subsequent works [16], [17], [18] propose algorithms that use determinized random sampling to build the search tree incrementally, with recent work addressing large observation spaces [17]. The use of  $\alpha$ -vectors in [16], [17], [18] relies on piecewise-linear approximations and thus only applies to POMDPs with belief-dependent rewards that admit such representations.

Previous methods start each planning session from scratch, while iX-BSP [19], [20] proposes reuse but assumes an open loop setting and does not address non-parametric beliefs. Sample reuse improves data efficiency in RL by leveraging past experiences [29]. Our approach instead uses online planning from a given belief, assuming known transition and observation models. Adaptive Belief Tree (ABT) [21] is an online POMDP solver for dynamic continuous-state domains that revises its particle-based belief tree upon model changes. It uses a generative transition model and assumes state-based rewards; the original formulation did not address continuous action and observation spaces, nor belief-dependent rewards. In this work, we address continuous state, action, and observation spaces with general belief-dependent rewards, a non-parametric framework, and a closed-loop setting.

### III. BACKGROUND

#### A. POMDP

POMDP is defined as a 7-tuple  $(S, A, O, \mathbb{P}_T, \mathbb{P}_O, r, b_0)$ , where  $S$ ,  $A$ , and  $O$  denote the state, action, and observation spaces. Since the exact state of the world is not known and only observations are available, the agent maintains a probability density function (PDF) over the state space—also referred to as the belief. The belief at time  $k$  is given by  $b_k(s_k) = \mathbb{P}(s_k | H_k)$ , where  $H_k = (b_0, a_0, o_1, \dots, o_k) = \{b_0, o_{1:k}, a_{1:k-1}\}$  denotes the history up to time  $k$ , consisting of the initial belief, the sequence

of observations, and the sequence of actions taken.  $\mathbb{P}_T$  is the state transition density function,  $\mathbb{P}_O$  is the observation density function,  $r(b, a, b')$  represents the reward function based on the current belief  $b$ , action  $a$ , and the resulting belief  $b'$ , and  $b_0$  denotes the initial belief over states. It is assumed that the belief is sufficient statistics for the decision making and a Bayesian update is used to update the belief recursively:

$$b_{k+1}(s_{k+1}) = \eta \mathbb{P}_O(o_{k+1} | s_{k+1}) \int_{s_k} \mathbb{P}_T(s_{k+1} | s_k, a_k) b_k(s_k) ds_k. \quad (1)$$

where  $\eta$  is a normalization term. A policy  $\pi \in \Pi$  is a mapping from belief space to action space  $\pi : b \rightarrow a$ . We define the value function  $V^\pi$  for any policy  $\pi$  and horizon  $d$  as

$$V^\pi(b_k) = \mathbb{E}_{b_{k+1:k+d}} [G_k | b_k, \pi]. \quad (2)$$

where  $\pi \triangleq \pi_{k:k+d-1}$  represents a sequence of policies for horizon  $d$  and  $G_k = \sum_{i=k}^{k+d-1} r(b_i, \pi_i(b_i), b_{i+1})$  is the return. Similarly, we define the action value function  $Q^\pi$  as

$$Q^\pi(b_k, a) = \mathbb{E}_{b_{k+1}} [r(b_k, a, b_{k+1}) + V^\pi(b_{k+1})]. \quad (3)$$

#### B. Non-Parametric Setting

We adopt a non-parametric setting, representing belief distributions with state particles. Using a particle filter [22], we update posterior estimates with each new observation. The theoretical belief  $b_k$  is approximated by  $m$  particles  $\{s_k^i\}_{i=1}^m$  assuming resampling, each with uniform weight  $\frac{1}{m}$

$$\hat{b}_k(s) = \frac{1}{m} \sum_{i=1}^m \delta(s - s_k^i). \quad (4)$$

Given resampled belief  $\hat{b}_k$ , action  $a_k$ , and propagated belief  $\hat{b}_{k+1}^-$ , calculating  $\mathbb{P}(\hat{b}_{k+1}^- | \hat{b}_k, a_k)$  involves determining all the matchings between the states in  $\hat{b}_k$  and those in  $\hat{b}_{k+1}^-$  which is  $\#P$ -complete [23]. We assume, similar to [24], that the beliefs are not permutation invariant, meaning particle beliefs with different particle orders are not considered identical. This assumption simplifies the derivation of the propagated belief likelihood. Consequently, we can express  $\hat{b}_k$  as  $\{s_k^i, \frac{1}{m}\}_{i=1}^m$  and  $\hat{b}_{k+1}^-$  as  $\{s_{k+1}^{-i}, \frac{1}{m}\}_{i=1}^m$

$$\mathbb{P}(\hat{b}_{k+1}^- | \hat{b}_k, a_k) = \frac{1}{m} \prod_{i=1}^m \mathbb{P}(s_{k+1}^{-i} | s_k^i, a_k). \quad (5)$$

In the rest of the paper we assume a non-parametric setting and for the ease of notation we remove the hat sign  $\hat{\cdot}$  and the state argument ( $s$ ) from all beliefs.

#### C. Importance Sampling

Importance sampling estimates properties of a target PDF  $p(x)$  by sampling from a proposal PDF  $q(x)$ , assigning weights to adjust each sample's contribution according to  $p(x)$

$$\hat{\mathbb{E}}_p^{IS}[f(x)] = \frac{1}{N} \sum_{i=1}^N w^i \cdot f(x^i), \quad w^i = \frac{p(x^i)}{q(x^i)}, \quad x^i \sim q. \quad (6)$$

The PDF  $q$  must satisfy  $q(x^i) = 0 \Rightarrow p(x^i) = 0$ . With  $M$  proposal PDFs  $\{q_m\}_{m=1}^M$ , Multiple Importance Sampling formulation [8] can be used:

$$\hat{\mathbb{E}}_p^{MIS}[f(x)] = \sum_{m=1}^M \frac{1}{n_m} \sum_{i=1}^{n_m} w^m(x^{i,m}) \frac{p(x^{i,m})}{q_m(x^{i,m})} f(x^{i,m}). \quad (7)$$

Here,  $n_m$  denotes the number of samples that originate from PDF  $q_m$ ,  $x^{i,m}$  denotes the  $i$ th sample that originates from PDF  $q_m$  and the weights  $w^m$  must satisfy

$$q_m(x^{i,m}) = 0 \Rightarrow w^m(x) f(x) p(x) = 0, \\ f(x^{i,m}) \neq 0 \Rightarrow \sum_{m=1}^M w^m(x^{i,m}) = 1, \quad (8)$$

ensuring that at least one PDF  $q_m(x) \neq 0$  for every valid  $x$ . Under these conditions, the estimator in (7) remains unbiased [8]. We assume that the weights  $w^m$  are determined using the balance heuristic which bounds the variance of the estimator [8] and in this case the MIS estimator is

$$\hat{\mathbb{E}}_p^{MIS}[f(x)] = \sum_{m=1}^M \sum_{i=1}^{n_m} \frac{p(x^{i,m})}{\sum_{j=1}^M n_j \cdot q_j(x^{i,m})} f(x^{i,m}). \quad (9)$$

For more details on MIS, see [8].

#### D. PFT-DPW

The PFT-DPW algorithm [10] is based on the UCT algorithm [9] and expands its application to a continuous state, action and observation setting. It utilizes Monte-Carlo simulations to progressively construct a policy tree for the belief MDP [10]. At every belief node  $b_k$  and action  $a_k$  it sets up visitation counts  $N(b_k, a_k)$  and  $N(b_k)$ , where  $N(b_k) = \sum_{a_k} N(b_k, a_k)$  and action-value function is calculated incrementally

$$Q(b_k, a_k) \triangleq \frac{1}{N} \sum_{i=1}^N G_k^i, \quad (10)$$

by averaging accumulated reward upon initiating from node  $b_k$  and taking action  $a_k$  within the tree. Notably,  $Q(b_k, a_k)$  (10) is not equal to  $Q^\pi(b_k, a_k)$  (3) as the policy varies across different simulations within the tree, causing the distribution of the trajectories to be non-stationary, hence the absence of the  $\pi$  superscript. The particle filter generates a propagate belief  $b_{k+1}^-$  and posterior belief  $b_{k+1}$  from  $b_k$  and  $a_k$ , sampling observation  $o_{k+1}$  and computing reward  $r$

$$b_{k+1}, b_{k+1}^-, o_{k+1}, r \leftarrow G_{PF(m)}(b_k, a_k). \quad (11)$$

To handle continuous spaces, Double Progressive Widening limits a node's children to  $kN^\alpha$ , where  $N$  is the node visit count, and  $k$  and  $\alpha$  are hyperparameters [10].

#### IV. APPROACH

Our contributions are threefold: (1) an efficient incremental update method for the Multiple Importance Sampling (MIS) estimator, enabling action-value estimation from prior and newly

arriving data; (2) the application of MIS for experience-based value estimation using expert-provided demonstrations without planning; and (3) an MCTS-inspired online algorithm that speeds up computations by reusing data from previous planning sessions.

##### A. Incremental Multiple Importance Sampling Update

In our setting, samples arrive incrementally in batches. A straightforward computation of (9) would necessitate a complexity of  $O(M^2 \cdot n_{avg})$ , where  $M$  denotes the number of different distributions and  $n_{avg}$  denotes the average sample count across all distributions. We develop an efficient way to update the estimator (9) incrementally in the theorem below.

*Theorem 1:* Consider an MIS estimator (9) with  $M$  different distributions and  $n_m$  samples for each distribution  $q_m \in \{q_1, \dots, q_M\}$ . Given a batch of  $L$  I.I.D samples from distribution  $q_{m'}$ , where  $q_{m'}$  could be one of the existing distributions or a new, previously unseen distribution,  $\hat{\mathbb{E}}_p^{MIS}[f(x)]$  (9) can be efficiently updated with a computational complexity of  $O(M \cdot n_{avg} + M \cdot L)$  and memory complexity  $O(M \cdot n_{avg})$ .

*Proof:* See Appendix A1.

##### B. Experience-Based Value Function Estimation

We assume that we have access to a dataset

$$D \triangleq \{\tau^i, G_{k_i}^i\}_{i=1}^{|D|} \quad (12)$$

of trajectories executed by an agent that followed an unknown policy  $\pi$ . Each trajectory is defined as the sequence

$$\tau^i \triangleq (b_{k_i}^i, a_{k_i}^i) \rightarrow (b_{k_i+1}^i, o_{k_i+1}^i, b_{k_i+1}^i, a_{k_i+1}^i) \rightarrow \dots \\ \rightarrow (b_{k_i+d}^i, o_{k_i+d}^i, b_{k_i+d}^i), \quad (13)$$

where  $k_i$  represents the starting time index and is used to differentiate between different steps in trajectory  $\tau^i$  and  $d$  is the horizon length. We assume that the agent applied a particle filter with resampling at each step of the trajectory. The return  $G^i$  associated with trajectory  $\tau^i$  is defined as the accumulated reward,

$$G_{k_i}^i \triangleq \sum_{j=0}^{d-1} r(b_{k_i+j}^i, a_{k_i+j}^i, b_{k_i+j+1}^i). \quad (14)$$

In this section, we evaluate  $V^\pi(b_k)$  for the current belief  $b_k$  using only the dataset  $D$  (12), without planning. Such estimation is important in data-expensive domains like autonomous vehicles [25] and robotic manipulation tasks [26]. In the next section, we will expand our methodology to include planning.

Reusing trajectories where the initial belief is set to  $b_k$  presents no challenge - we can aggregate all trajectories that begin with belief  $b_k$  and action  $a_k$  and assuming we have  $N$  such trajectories, we define a sample-based estimator

$$\hat{Q}^\pi(b_k, a_k) \triangleq \frac{1}{N} \sum_{i=1}^N G_k^i. \quad (15)$$

In continuous spaces, the chance of sampling the same belief twice is zero, so each trajectory in  $D$  (12) begins from a belief

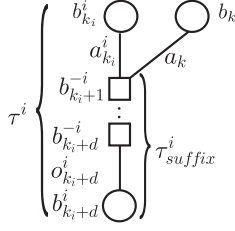


Fig. 1.  $\tau^i$  is a trajectory that was executed by an agent that followed policy  $\pi$ ,  $\tau_{suffix}^i$  is the part that we reuse from  $\tau^i$  for the current belief  $b_k$  and action  $a_k$ .

different from  $b_k$ . To be able to reuse trajectories from (12), we discard the initial belief and action of the trajectory, instead linking the current belief and action to the remainder of the trajectory. Formally, given a trajectory  $\tau^i \in D$ ,  $\tau^i = (b_{k_i}^i, a_{k_i}^i) \rightarrow \tau_{suffix}^i$  where

$$\begin{aligned} \tau_{suffix}^i &\triangleq (b_{k_i+1}^{-i}, o_{k_i+1}^i, b_{k_i+1}^i, a_{k_i+1}^i) \rightarrow \dots \\ &\rightarrow (b_{k_i+d}^{-i}, o_{k_i+d}^i, b_{k_i+d}^i). \end{aligned} \quad (16)$$

and the current belief  $b_k$  and action  $a_k$ , we construct a new trajectory  $\tau_i'$  (see Figure 1),

$$\tau_i' \triangleq (b_k, a_k) \rightarrow \tau_{suffix}^i. \quad (17)$$

To estimate  $Q^\pi(b_k, a_k)$  using the information within trajectory  $\tau^i$ , two adjustments are required. Firstly, we need to modify the initial term in the return  $G^i$  to be equal to  $r(b_k, a_k, b_{k_i+1}^i)$ , recognizing that  $b_k \neq b_{k_i}^i$  and  $a_k \neq a_{k_i}^i$ . Consequently, we define the return of trajectory

$$\tilde{G}_k^i \triangleq G_{k_i}^i - r(b_{k_i}^i, a_{k_i}^i, b_{k_i+1}^i) + r(b_k, a_k, b_{k_i+1}^i). \quad (18)$$

Secondly, we need to adjust the weight of  $\tilde{G}_k^i$  due to the disparity between  $\mathbb{P}(\tau_{suffix}^i | b_{k_i}^i, a_{k_i}^i, \pi)$  and  $\mathbb{P}(\tau_{suffix}^i | b_k, a_k, \pi)$ , which is achieved through importance sampling. The distribution  $\mathbb{P}(\cdot | b_{k_i}^i, a_{k_i}^i, \pi)$  of  $\tau_{suffix}^i$  (16) is determined by the initial belief  $b_{k_i}^i$  and action  $a_{k_i}^i$ . Given  $N_{IS}$  partial trajectories sampled from the same distribution  $\mathbb{P}(\cdot | b_{k_i}^i, a_{k_i}^i, \pi)$ , we define an Importance Sampling estimator

$$\hat{Q}_{IS}^\pi(b_k, a_k) \triangleq \frac{1}{N_{IS}} \sum_{i=1}^{N_{IS}} w^i \cdot \tilde{G}_k^i. \quad (19)$$

where  $w^i \triangleq \frac{\mathbb{P}(\tau_{suffix}^i | b_k, a_k, \pi)}{\mathbb{P}(\tau_{suffix}^i | b_{k_i}^i, a_{k_i}^i, \pi)}$ . As a result of our approach to constructing reusable trajectories as described in (17), we can efficiently calculate the weights  $w^i$  utilizing the theorem presented below.

**Theorem 2:** Given belief node  $b_k$ , action  $a_k$  and trajectory  $\tau^i = (b_{k_i}^i, a_{k_i}^i) \rightarrow \tau_{suffix}^i$  where  $\tau_{suffix}^i$  is defined in (16), the following equality holds:

$$\frac{\mathbb{P}(\tau_{suffix}^i | b_k, a_k, \pi)}{\mathbb{P}(\tau_{suffix}^i | b_{k_i}^i, a_{k_i}^i, \pi)} = \frac{\mathbb{P}(b_{k_i+1}^{-i} | b_k, a_k)}{\mathbb{P}(b_{k_i+1}^{-i} | b_{k_i}^i, a_{k_i}^i)}. \quad (20)$$

*Proof:* See Appendix A2.

Let  $M$  be the number of unique partial trajectory PDFs  $\{\mathbb{P}(\cdot | b_{k_m}^m, a_{k_m}^m, \pi)\}_{m=1}^M$  each defined by its initial belief  $b_{k_m}^m$

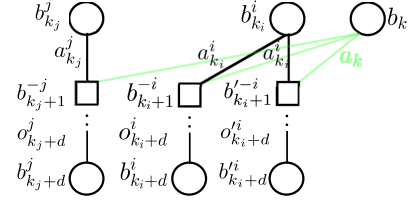


Fig. 2. Illustration of reuse of three trajectories.

and action  $a_{k_m}^m$ , and let  $n_m$  denote the sample count for each. Consequently, the dataset  $D$  (12) can be reformulated as follows:

$$D \triangleq \{\tau^{l,m}, G_k^{l,m}\}_{m=1, l=1}^{M, n_m}. \quad (21)$$

Using this formulation, we define a multiple importance sampling estimator assuming the balance heuristic (9),

$$\hat{Q}_{MIS}^\pi(b_k, a_k) \triangleq \sum_{m=1}^M \sum_{l=1}^{n_m} \frac{\mathbb{P}(\tau_{suffix}^{l,m} | b_k, a_k, \pi) \tilde{G}_k^{l,m}}{\sum_{j=1}^M n_j \cdot \mathbb{P}(\tau_{suffix}^{l,m} | b_{k_j}^j, a_{k_j}^j, \pi)}. \quad (22)$$

where  $\tau_{suffix}^{l,m}$  represents the  $l$ th partial trajectory that was sampled from the distribution  $\mathbb{P}(\cdot | b_{k_m}^m, a_{k_m}^m, \pi)$  and  $\tilde{G}_k^{l,m}$  is the adjusted accumulated reward (18).

Using Theorem 2, we can re-write the MIS estimator (22)

$$\hat{Q}_{MIS}^\pi(b_k, a_k) \triangleq \sum_{m=1}^M \sum_{l=1}^{n_m} \frac{\mathbb{P}(b_{k_m+1}^{-l,m} | b_k, a_k)}{\sum_{j=1}^M n_j \cdot \mathbb{P}(b_{k_m+1}^{-l,m} | b_{k_j}^j, a_{k_j}^j)} \cdot \tilde{G}_k^{l,m}. \quad (23)$$

Since each element in the second sum of (23) corresponds to a propagated belief, which might appear more than once, we can rewrite the sum in a more compact form. Specifically, we group the terms based on unique propagated beliefs and account for their multiplicity:

$$\begin{aligned} \hat{Q}_{MIS}^\pi(b_k, a_k) &\triangleq \sum_{m=1}^M \sum_{l=1}^{|C(b_{k_m}, a_{k_m})|} W(b_{k_m+1}^{-l,m}) \cdot \\ &\sum_{y=1}^{N(b_{k_m+1}^{-l,m})} \tilde{G}_k^{m,l,y}. \end{aligned} \quad (24)$$

The weights  $W(b_{k_m+1}^{-l,m})$  are defined by:

$$W(b_{k_m+1}^{-l,m}) = \frac{\mathbb{P}(b_{k_m+1}^{-l,m} | b_k, a_k)}{\sum_{j=1}^M n_j \cdot \mathbb{P}(b_{k_m+1}^{-l,m} | b_{k_j}^j, a_{k_j}^j)} \quad (25)$$

$C(b_{k_m}, a_{k_m})$  denotes the set of reused propagated belief children associated with  $b_{k_m}$  and  $a_{k_m}$ . The term  $N(b_{k_m+1}^{-l,m})$  represents the visitation count of  $b_{k_m+1}^{-l,m}$ , indicating the number of trajectories that pass through the propagated belief  $b_{k_m+1}^{-l,m}$  and  $\tilde{G}_k^{m,l,y}$  is the return of the  $y$ -th trajectory passing through  $b_{k_m+1}^{-l,m}$ . Note that  $b_{k_m+1}^{-l,m}$  in (24) represents unique propagated beliefs, which differs from (23), where it denotes the propagated belief associated with a single trajectory. Figure 2 illustrates the estimator from (24). For the current belief  $b_k$  and action  $a_k$ , three prior



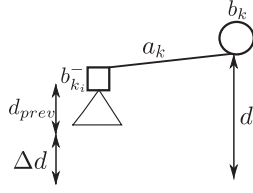


Fig. 3. Illustration of horizon gap.

trajectories are incorporated: two from  $(b_{k_i}^i, a_{k_i}^i)$  and one from  $(b_{k_j}^j, a_{k_j}^j)$ . Light green edges show the connections between  $(b_k, a_k)$  and the reused nodes for estimating  $\hat{Q}_{MIS}^\pi(b_k, a_k)$ . Further in this work, we consider a framework where the dataset  $D$  (21) expands over time with trajectory samples from an agent following policy  $\pi$ . Theorem 1 is used to efficiently update the estimator (23) with new samples.

For the estimator in (24) to be unbiased, the conditions in (8) must hold. Specifically, for every propagated belief  $b_{k+1}^-$  that can be generated from  $b_k, a_k$ , there must exist at least one pair  $b_{k_j}^j, a_{k_j}^j$  from which  $b_{k+1}^-$  can also be generated.

Our framework differs from standard off-policy evaluation. Traditional importance sampling estimates  $V^{\pi_i}(b_k)$  using trajectories from  $b_k$  under a behavior policy  $\pi_b$  [27]. In contrast, we estimate  $V^\pi(b_k)$  using trajectories from *different* beliefs in the dataset  $D$  (12). To our knowledge, such a setting has not been previously explored for action-value estimation in POMDPs.

### C. Our POMDP Planning Algorithm: IR-PFT

Thus far, we used trajectories from a single policy  $\pi$  to estimate  $Q^\pi(b_k, a_k)$ . In this section, we introduce an anytime POMDP planning algorithm that accelerates planning by reusing trajectories from dataset  $D$ , which contains data from prior planning sessions.

We name our algorithm Incremental Reuse Particle Filter Tree (IR-PFT). Instead of calculating  $Q(b_k, a_k)$  from scratch in each planning session, we use previous experience to speed up the calculations.

We adopt the same approach as in Section IV-B to reuse trajectories, with three key modifications: first, the propagated belief nodes from the previous planning session in dataset  $D$  have a shorter planning horizon. We extend the horizon of these nodes before reusing them; second, the policy varies across different simulations (as in standard MCTS), resulting in a non-stationary distribution of reused trajectories in  $D$ ; and third, we integrate the planning and generation of new trajectories with the reuse of previous trajectories within an anytime MCTS setting. Fig. 3 visually illustrates the horizon alignment process, where a propagated belief node  $b_{k_i}^-$  with horizon  $d_{prev}$  must be extended by  $\Delta d$  to match the current horizon  $d$ . We analyze the complexity of the correction of belief nodes from previous planning sessions in case of using the MCTS [28] algorithm in Corollary 1.

*Corollary 1:* Given an MCTS tree  $T$  with horizon  $d_{prev}$ , number of simulations  $m$  and  $N$  nodes, extending its horizon by  $\Delta d$  will require adding at most  $m \cdot \Delta d$  nodes and reward calculations.

The proof is straightforward: after  $m$  simulations, the MCTS tree contains at most  $m$  leaves and we need to extend each leaf by  $\Delta d$  and for each new node we calculate a reward.

We now define the estimator

$$\hat{Q}_{MIS}(b_k, a_k) \triangleq \sum_{m=1}^M \sum_{l=1}^{|C(b_{k_m}, a_{k_m})|} W(b_{k_m+1}^{-l,m}) \cdot \sum_{y=1}^{N(b_{k_m+1}^{-l,m})} \bar{G}_k^{m,l,y}, \quad (26)$$

where the weights  $W(b_{k_m+1}^{-l,m})$  are defined in (25).  $\bar{G}_k^{m,l,y}$  is the extended return defined as

$$\bar{G}_k^{m,l,y} = \tilde{G}_k^{m,l,y} + \sum_{i=k+d_{prev}^{l,m}}^{k+d_{prev}^{l,m}+\Delta d-1} r(b_i, \pi_{rollout}(b_i), b_{i+1}). \quad (27)$$

$d_{prev}^{l,m}$  is the horizon of propagated belief  $b_{k_m+1}^{-l,m}$ ,  $\bar{G}_k^{m,l,y}$  shares the same values in the summation as the return  $\tilde{G}_k^{m,l,y}$  (18), but it also includes additional terms from the extended trajectory due to the horizon extension using the rollout policy  $\pi_{rollout}$ . Therefore, only the rewards for these additional terms need to be computed when extending the horizon, while all shared terms ( $\tilde{G}_k^{m,l,y}$ ) can be reused.

Since the tree policy in MCTS differs across simulations, the resulting trajectory distribution becomes non-stationary. As a consequence, the update defined in (26) functions in a heuristic manner, and its convergence properties remain unproven. We leave a rigorous investigation of this aspect for future work.

After extending the horizon of a reused propagated belief node  $b^-$  and reusing its action-value function, the counter  $N(b_k, a_k)$  is incremented by the visitation count  $N(b^-)$  using the relation  $N(b_k, a_k) = \sum_{b_k^- \in C(b_k, a_k)} N(b_k^-)$ . This approach accelerates our algorithm for a given number of simulations, offering a speedup over PFT-DPW [10].

To summarize, here is the high-level logical flow of our algorithm: At each iteration, we either reuse a propagated belief node by extending its horizon by  $\Delta d$ , as illustrated in Figure 3, and compute the extended return for the subtree rooted at the reused node  $b^-$ , or create a new node. Subsequently, the Multiple Importance Sampling (MIS) estimator (26) is employed to evaluate the action-value function. To avoid the computational expense of a naive calculation, we leverage Theorem 1 to perform efficient incremental updates of the estimator in (26).

### D. Algorithm Description

The complete algorithm is outlined across multiple methods - Algs. 1, 2, 3 and 4. Alg. 1 illustrates a general planning loop wherein the agent iteratively plans and executes actions until the problem is solved. After each planning session, reuse candidates are updated based on the preceding planning tree.

The main algorithm is detailed in Alg. 2 with key modifications compared to the PFT-DPW algorithm [10] highlighted in red. The ActionProgWiden method (line 12) is implemented

**Algorithm 1** General Planning Loop.

---

```

1: Procedure: SOLVE( $b, D$ )
2: while ProblemNotSolved() do
3:    $a \leftarrow \text{Plan}(b, D)$ 
4:    $o \leftarrow \text{ReceiveObservation}(b, a)$ 
5:    $b', b^-, r \leftarrow G_{PF(m)}(b, a, o)$ 
6:   UpdateReuseCandidates( $a, D, b, b'$ )
7:    $b \leftarrow b'$ 
8: end while

```

---

following the same approach as described in [10]. ShouldReuse method (line 14) evaluates three conditions: current node  $b$  is the root, the balance between reused and new nodes, and the availability of reuse candidates. The second criterion is important because, while acquiring estimates from prior partial trajectories is runtime-efficient, generating new trajectory samples from the correct distribution is essential. Currently, reuse is applied only at the root node, where it yields the greatest computational savings by avoiding many reward computations due to its shallow depth. While extending reuse to nodes at other depth levels is feasible, it falls outside the scope of this work.

The GetReuseCandidate method (line 15) selects a candidate propagated belief  $b'^-$  from dataset  $D$  using a distance function  $f_D$  (line 24). For example,  $f_D$  may be defined as  $\|b^- - b_{MLE}^-\|_2^2$ , where  $b_{MLE}^-$ —the maximum likelihood propagated belief for given  $b$  and  $a$ —is computed via (5) in  $O(m)$  time. Since  $f_D$  scans the entire dataset, it must be efficient, and reusing nodes with high visitation counts further reduces runtime.

The FillHorizonPropagated method (line 16), addresses discrepancies in horizon lengths when reusing nodes from the previous planning sessions. Algorithm 4 performs recursive traversal of the subtree defined by propagated belief  $b'^-$  and extends its depth by  $d$  using the rollout policy.

At lines 17 and 18, we increment counters, where  $N(b'^-)$  represents the count of trajectories passing through reuse candidate propagated belief node  $b'^-$ . At line 19, we increment the PLAN procedure counter by  $N(b'^-)$ .

At lines 20 and 36 we utilize (26) to update  $Q(b, a)$ , leveraging efficiency through the application of Theorem (1). At line 21 we store the propagated belief  $b'^-$ .

Lines 24–26 execute when reuse is skipped: they initialize a new propagated belief via the particle filter [22], save the propagated and posterior beliefs, and perform a rollout.

At lines 30 and 31 we sample uniformly both propagated and posterior beliefs.

In Algorithm 3, UpdateReuseCandidates selects nodes with more than  $n_{min}$  visits to maximize speedup.

## V. RESULTS

We assess the performance of the IR-PFT algorithm by comparing it to the PFT-DPW algorithm [10]. Our evaluation focuses on two main aspects: runtime and accumulated reward, with statistics measured for each. In all experiments, the solvers were limited to 1000 iterations for each planning phase. All

**Algorithm 2** IR-PFT.

---

```

1: Procedure: PLAN( $b, D$ )
2:  $i = 0$ 
3: while  $i < n$  do
4:    $\text{Simulate}(b, d_{max}, D)$ 
5: end while
6:  $a = \text{argmax}_a \{Q(b, a)\}$ 
7: return  $a$ 

```

---

```

1: Procedure: SIMULATE( $b, d, D$ )
2: if  $d = 0$  then
3:   return 0
4: end if
5:  $a \leftarrow \text{ActionProgWiden}(b)$ 
6: if  $|C(ba)| \leq k_o N(ba)^{\alpha_o}$  then
7:   if ShouldReuse( $b, a, D$ ) then
8:      $b'^- \leftarrow \text{GetReuseCandidate}(b, a, D)$ 
9:     FillHorizonPropagated( $b'^-, d - d_{b^-}$ )
10:     $N(b) \leftarrow N(b) + N(b'^-)$ 
11:     $N(ba) \leftarrow N(ba) + N(b'^-)$ 
12:     $i \leftarrow i + N(b'^-)$  {update simulation counter}
13:     $Q(ba) \leftarrow \text{MISUupdate}$  defined by eq. (26)
14:     $C(b, a) \leftarrow C(b, a) \cup \{(b'^-)\}$ 
15:    return  $Q(ba)$ 
16:  else
17:     $b', b^-, r \leftarrow G_{PF(m)}(b, a)$ 
18:     $C(b, a) \leftarrow C(b, a) \cup \{(b'^-)\}$ 
19:     $C(b'^-) \leftarrow C(b'^-) \cup \{(b', r)\}$ 
20:     $total \leftarrow r + \gamma \text{ROLLOUT}(b', d - 1)$ 
21:  end if
22: else
23:    $b'^- \leftarrow \text{sample uniformly from } C(ba)$ 
24:    $b', r \leftarrow \text{sample uniformly from } C(b'^-)$ 
25:    $total \leftarrow r + \gamma \text{Simulate}(b', d - 1, T)$ 
26: end if
27:  $N(b) \leftarrow N(b) + 1$ 
28:  $N(ba) \leftarrow N(ba) + 1$ 
29:  $Q(ba) \leftarrow \text{MISUupdate}$  defined by eq. (26)
30: return  $total$ 

```

---

experiments were conducted on the standard 2D Light Dark benchmark, where the agent must reach the goal while minimizing localization uncertainty. Beacons define illuminated regions, where observation noise decreases linearly outside them, reaching a minimum at the specified white radius, while areas beyond are considered dark. Refer to the illustration in Fig. 4(a). The reward function is defined as a weighted sum of the average distance to goal and differential entropy estimator which is calculated using [7]. Each algorithm was evaluated using different quantities of particles—specifically, 5, 10, 15, and 20, while maintaining a constant horizon length of  $d = 10$ . In the following results reuse was done according to ShouldReuse method (line 14) as detailed in the previous section. We compared the performance of IR-PFT (with and without reuse) to PFT-DPW and present the findings as a speedup chart

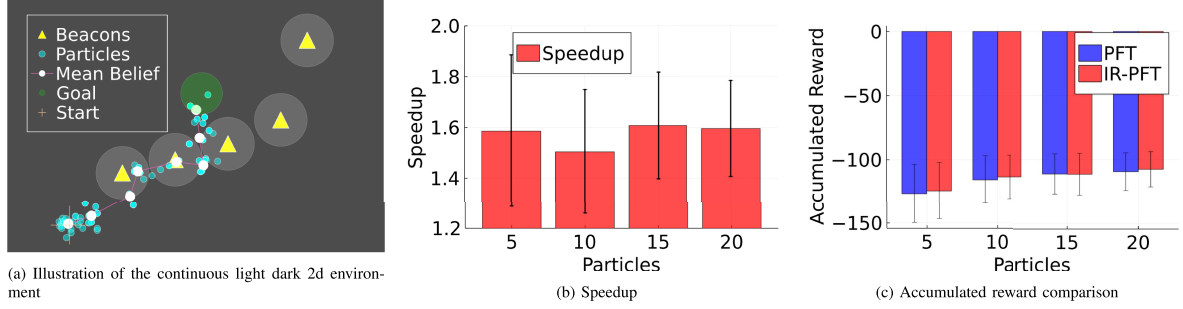


Fig. 4. Light dark experiments comparing PFT and IR-PFT.

#### Algorithm 3 Reuse Functions.

```

1: Procedure: UPDATEREUSECANDIDATES( $a, D, b_k, b_{k+1}^{real}$ )
2: ReuseDict  $dict \leftarrow \{\}$ 
3: for  $b_{k+1}^- \in C(b_k, a)$  do
4:   for  $b_{k+1}^- \in C(b_{k+1}^-)$  do
5:     for  $a' \in Actions(b_{k+1})$  do
6:       for  $b_{k+2}^- \in C(b_{k+1}, a')$  do
7:         if  $N(b_{k+2}^-) > n_{min}$  then
8:            $D.append(b_{k+2}^-)$ 
9:         end if
10:      end for
11:    end for
12:  end for
13: end for

1: Procedure: SHOULDREUSE( $b, a, D$ )
2: if not  $b.IsRoot()$  then
3:   return false
4: end if
5: if  $NumReused(b, a) > \frac{|C(b, a)|}{2}$  then
6:   return false
7: end if
8:  $candidates \leftarrow D.GetReuseCandidatesDict()$ 
9: return not( $candidates.empty()$ )

1: Procedure: GETREUSECANDIDATE( $b, a, D$ )
2:  $b^- \leftarrow argmin_{b^-} \{f_D(b^-, b, a)\}$ 
3: return  $b^-$ 

```

#### Algorithm 4 Fill Horizon Gap.

```

1: Procedure: FILLHORIZONPROPAGATED( $b^-, d$ )
2:  $Q_{new}(b^-) \leftarrow 0$ 
3: for  $b' \in C(b^-)$  do
4:    $Q_{new}(b^-) \leftarrow$ 
      $Q_{new}(b^-) + FillHorizonPosterior(b')$ 
5: end for
6: return  $Q_{new}(b^-)$ 

1: Procedure: FILLHORIZONPOSTERIOR( $b, d$ )
2: if  $IsLeaf(b)$  then
3:    $a \leftarrow DefaultPolicy(b)$ 
4:    $b', b'^-, r \leftarrow G_{PF(m)}(b, a)$ 
5:    $N(b, a) \leftarrow 1$ 
6:    $N(b'^-) \leftarrow 1$ 
7:    $Q(b'^-) \leftarrow r$ 
8:    $Q(b, a) \leftarrow r$ 
9:   return  $r$ 
10: end if
11:  $Q(b) \leftarrow 0$ 
12: for  $a \in Actions(b)$  do
13:   for  $b'^- \in C(b, a)$  do
14:      $Q(b) \leftarrow$ 
        $Q(b) + FillHorizonPropagated(b'^-, d - 1)$ 
15:   end for
16: end for
17:  $Q(b) \leftarrow \frac{Q(b)}{N(b)}$ 
18: return  $Q(b)$ 

```

in Fig. 4(b), plotted against the number of particles. IR-PFT consistently outperformed PFT-DPW, with the speedup saturating at approximately 1.5—a factor primarily attributed to the savings in reward computation, which is the most computationally intensive part of the algorithm. We compare the accumulated rewards of IR-PFT with and without reuse (Fig. 4(c)). The results show negligible differences, indicating that our method improves runtime without compromising planning performance.

## VI. CONCLUSION

In this letter, we have proposed a general framework which allows to reuse prior information during the current planning session. We derived theoretical justification for reuse via Multiple

Importance Sampling and introduced a new MCTS-like algorithm, IR-PFT which reuses information from previous planning session and allows to speed up calculations in current planning session. In order to evaluate IR-PFT algorithm, we conducted an empirical performance study. Specifically, we compared the performance of our approach with and without the reuse of prior information. We measured various performance metrics, including computation time and the accumulated reward. Our results clearly indicate a speed-up in the planning process when prior information is leveraged. Importantly, despite the accelerated computations, our approach maintains the same level of performance as the traditional planning approach without reuse. Incorporating prior information significantly boosts planning

efficiency, delivering time savings while maintaining high-quality results. These findings underscore the effectiveness and potential of the proposed approach. Scaling to higher dimensions is challenging, as similar belief states become exponentially rarer. However, imposing structural assumptions may still allow reuse, as shown in [20].

## APPENDIX A

### A1 Proof of Theorem 1

Consider an MIS estimator (9) with  $M$  different distributions and  $n_m$  samples for each distribution  $q_m \in \{q_1, \dots, q_M\}$ . Given a batch of  $L$  I.I.D. samples from distribution  $q_{m'}$  which may be an existing or new distribution,

$$\hat{\mathbb{E}}_p^{MIS}[f(x)] = \sum_{m=1}^M \sum_{i=1}^{n_m} \frac{p(x_{i,m})}{\sum_{j=1}^M n_j \cdot q_j(x_{i,m})} f(x_{i,m}),$$

Equation (9) can be efficiently updated with a computational complexity of  $O(M \cdot n_{avg} + M \cdot L)$  and memory complexity  $O(M \cdot n_{avg})$ .

For every distribution  $q_m$  we have the term  $\sum_{i=1}^{n_m} \frac{p(x_{i,m})}{\sum_{j=1}^M n_j \cdot q_j(x_{i,m})} f(x_{i,m})$ .

In case  $m \neq m'$ :

$\sum_{i=1}^M n_j \cdot q_j(x_{i,m}) \leftarrow \sum_{j=1}^M n_j \cdot q_j(x_{i,m}) + L \cdot q_{m'}(x_{i,m})$  -  $O(1)$  complexity. We have  $n_m$  samples and  $M$  distributions so the complexity of this update is  $O(M \cdot n_m)$ .

In case  $m = m'$ :

For existing samples  $\sum_{j=1}^M n_j \cdot q_j(x_{i,m}) \leftarrow \sum_{j=1}^M n_j \cdot q_j(x_{i,m}) + L \cdot q_{m'}(x_{i,m})$  -  $O(1)$  complexity. We have  $n_m$  samples existing samples so in total  $O(n_m)$  complexity.

For each new sample we need to calculate  $\frac{p(x_{i,m})}{\sum_{j=1}^M n_j \cdot q_j(x_{i,m})} f(x_{i,m})$  -  $O(M)$  complexity. We have  $L$  new samples so in total  $O(L \cdot M)$  complexity. The total complexity of the update is  $O(M \cdot n_{avg} + M \cdot L)$ .

### A2 Proof of Theorem 2

$$\frac{\mathbb{P}(\tau_{suffix}^i | b_k, a_k, \pi)}{\mathbb{P}(\tau_{suffix}^i | b_{k_i}^i, a_{k_i}^i, \pi)} = \frac{\mathbb{P}(b_{k_i+1}^{-i}, \dots, b_{k_i+L}^i | b_k, a_k, \pi)}{\mathbb{P}(b_{k_i+1}^{-i}, \dots, b_{k_i+L}^i | b_{k_i}^i, a_{k_i}^i, \pi)}. \quad (28)$$

Applying chain rule yields,

$$\begin{aligned} & \frac{\mathbb{P}(b_{k_i+1}^{-i} | b_k, a_k)}{\mathbb{P}(b_{k_i+1}^{-i} | b_{k_i}^i, a_{k_i}^i)} \cdot \frac{\mathbb{P}(o_{k_i+1}^i, \dots, b_{k_i+L}^i | b_{k_i+1}^{-i}, \pi)}{\mathbb{P}(o_{k_i+1}^i, \dots, b_{k_i+L}^i | b_{k_i+1}^{-i}, \pi)} \\ &= \frac{\mathbb{P}(b_{k_i+1}^{-i} | b_k, a_k)}{\mathbb{P}(b_{k_i+1}^{-i} | b_{k_i}^i, a_{k_i}^i)}. \end{aligned} \quad (29)$$

## REFERENCES

- [1] C. Papadimitriou and J. Tsitsiklis, "The complexity of Markov decision processes," *Math. Operations Res.*, vol. 12, no. 3, pp. 441–450, 1987.
- [2] D. Silver and J. Veness, "Monte-Carlo planning in large POMDPs," in *Proc. Adv. Neural Inf. Process. Syst.*, 2010, pp. 2164–2172.
- [3] A. Somani, N. Ye, D. Hsu, and W. S. Lee, "DESPOT: Online POMDP planning with regularization," in *Proc. Adv. Neural Inf. Process. Syst.*, 2013, vol. 13, pp. 1772–1780.
- [4] M. Hoerger and H. Kurniawati, "An on-line POMDP solver for continuous observation spaces," in *Proc. IEEE Int. Conf. Robot. Automat.*, 2021, pp. 7643–7649.
- [5] M. Araya-López, O. Buffet, V. Thomas, and F. Charpillet, "A POMDP extension with belief-dependent rewards," in *Proc. Neural Inf. Process. Syst.*, 2010, pp. 64–72.
- [6] J. Fischer and O. S. Tas, "Information particle filter tree: An online algorithm for POMDPs with belief-based rewards on continuous domains," in *Proc. Int. Conf. Mach. Learn.*, 2020, pp. 3177–3187.
- [7] Y. Boers, H. Driessen, A. Bagchi, and P. Mandal, "Particle filter based entropy," in *Proc. 2010 13th Int. Conf. Inf. Fusion*, 2010, pp. 1–8.
- [8] E. Veach and L. J. Guibas, "Optimally combining sampling techniques for Monte Carlo rendering," in *Proc. 22nd Annu. Conf. Comput. Graph. Interactive Techn.*, 1995, pp. 419–428.
- [9] L. Kocsis and C. Szepesvári, "Bandit based Monte-Carlo planning," in *Proc. Eur. Conf. Mach. Learn.*, 2006, pp. 282–293.
- [10] Z. Sunberg and M. Kochenderfer, "Online algorithms for POMDPs with continuous state, action, and observation spaces," in *Proc. Int. Conf. Automated Plan. Scheduling*, 2018, vol. 28, no. 1, pp. 259–263.
- [11] V. Thomas, G. Hutin, and O. Buffet, "Monte Carlo information-oriented planning," 2021, *arXiv:2103.11345*.
- [12] O. Szttyglic and V. Indelman, "Speeding up online POMDP planning via simplification," in *Proc. IEEE/RSJ Int. Conf. Intell. Robots Syst.*, 2022, pp. 7174–7181.
- [13] A. Zhitnikov, O. Szttyglic, and V. Indelman, "No compromise in solution quality: Speeding up belief-dependent continuous POMDPs via adaptive multilevel simplification," *Int. J. Robot. Res.*, vol. 44, pp. 157–195, 2024.
- [14] M. Barenboim and V. Indelman, "Adaptive information belief space planning," in *Proc. 31st Int. Joint Conf. Artif. Intell. 25th Eur. Conf. Artif. Intell.*, 2022, pp. 4588–4596.
- [15] A. Zhitnikov and V. Indelman, "Simplified risk aware decision making with belief dependent rewards in partially observable domains," in *Proc. Thirty-Second Int. Joint Conf. Artif. Intell.*, E. Elkind, Ed., International Joint Conferences on Artificial Intelligence Organization, Aug. 2023, vol. 312, pp. 7001–7005. doi: [10.24963/ijcai.2023/798](https://doi.org/10.24963/ijcai.2023/798).
- [16] N. Ye, A. Somani, D. Hsu, and W. S. Lee, "DESPOT: Online POMDP planning with regularization," *J. Artif. Intell. Res.*, vol. 58, pp. 231–266, 2017.
- [17] N. P. Garg, D. Hsu, and W. S. Lee, "DESPOT- $\alpha$ : Online POMDP planning with large state and observation spaces," in *Proc. Robot.: Sci. Syst.*, 2019 doi: [10.15607/RSS.2019.XV.006](https://doi.org/10.15607/RSS.2019.XV.006).
- [18] P. Cai, Y. Luo, D. Hsu, and W. S. Lee, "HyP-DESPOT: A hybrid parallel algorithm for online planning under uncertainty," *Int. J. Robot. Res.*, vol. 40, no. 2–3, pp. 558–573, 2021.
- [19] E. I. Farhi and V. Indelman, "iX-BSP: Belief space planning through incremental expectation," in *Proc. IEEE Int. Conf. Robot. Automat.*, 2019, pp. 7180–7186.
- [20] E. Farhi and V. Indelman, "iX-BSP: Incremental belief space planning," 2021, *arXiv:2102.09539*.
- [21] H. Kurniawati and V. Yadav, "An online POMDP solver for uncertainty planning in dynamic environment," in *Robotics Research*. New York, NY, USA: Springer, 2016, pp. 611–629.
- [22] S. Thrun, W. Burgard, and D. Fox, *Probabilistic Robotics*. Cambridge, MA, USA: MIT Press, 2005.
- [23] L. G. Valiant, "The complexity of computing the permanent," *Theor. Comput. Sci.*, vol. 8, no. 2, pp. 189–201, Apr. 1979.
- [24] M. H. Lim, T. J. Becker, M. J. Kochenderfer, C. J. Tomlin, and Z. N. Sunberg, "Optimality guarantees for particle belief approximation of POMDPs," *J. Artif. Intell. Res.*, vol. 77, pp. 1591–1636, 2023.
- [25] K. T. E. A. H. Caesar and J. Kabzan, "NuPlan: A closed-loop ML-based planning benchmark for autonomous vehicles," in *Proc. Conf. Comput. Vis. Pattern Recognit. ADP3 Workshop*, 2021.
- [26] A. Mandelkar et al., "Scaling robot supervision to hundreds of hours with roboturk: Robotic manipulation dataset through human reasoning and dexterity," in *Proc. IEEE/RSJ Int. Conf. Intell. Robots Syst.*, 2019, pp. 1048–1055.
- [27] R. S. Sutton and A. G. Barto, *Reinforcement Learning: An Introduction*. Cambridge, MA, USA: MIT Press, 2018.
- [28] D. Auger, A. Couetoux, and O. Teytaud, "Continuous upper confidence trees with polynomial exploration - consistency," in *Proc. Eur. Conf. Mach. Learn.*, 2013, pp. 194–209.
- [29] V. Mnih et al., "Human-level control through deep reinforcement learning," *Nature*, vol. 518, no. 7540, pp. 529–533, 2015.